

# Cotunneling Spectroscopy in Few-Electron Quantum Dots

D. M. Zumbühl and C. M. Marcus

*Department of Physics, Harvard University, Cambridge, Massachusetts 02138*

M. P. Hanson and A. C. Gossard

*Materials Department, University of California, Santa Barbara, California 93106*

Few-electron quantum dots are investigated in the regime of strong tunneling to the leads. Inelastic cotunneling is used to measure the two-electron singlet-triplet splitting above and below a magnetic field driven singlet-triplet transition. Evidence for a non-equilibrium two-electron singlet-triplet Kondo effect is presented. Cotunneling allows orbital correlations and parameters characterizing entanglement of the two-electron singlet ground state to be extracted from dc transport.

Transport studies of few-electron quantum dots have proven to be a rich laboratory for investigating the energetics of electrons in artificial atoms [1, 2, 3] as well as related spin effects, including ground-state spin transitions [4, 5, 6, 7], spin lifetimes [6, 7, 8] and Kondo effects [9, 10, 11]. The interplay of electron-electron interactions, electron spin, and coupling to a Fermi sea makes transport in the few-electron regime a subtle problem in many-body physics [12, 13, 14, 15, 16, 17]. Of particular importance is the two-electron case (“quantum dot helium”) [17] since this is a paradigm for the preparation of entangled electronic states [18], and in double quantum dots is the basis of a quantum gate proposal [19].

In this Letter, we present a detailed experimental investigation of cotunneling through quantum dots containing one, two, and three electrons. Measurements of inelastic cotunneling are used to extract the singlet-triplet (ST) splitting across the two-electron ST transition. Evidence of a non-equilibrium ST Kondo effect for two electrons is presented. Cotunneling and Kondo effects are used to determine the  $g$ -factor for magnetic fields along different directions in the plane of the 2D electron gas (2DEG), giving isotropic  $g$ -factors close to the bulk GaAs value. Using both cotunneling and sequential tunneling data, we extract quantum correlations of the two-electron singlet ground state, allowing the degree of spatially separated entanglement to be measured.

Previous transport studies of few-electron quantum dots have identified the ST ground state transition for two electrons [2, 3, 4, 5, 6] as well as for larger electron numbers [20, 21]. Inelastic cotunneling was recently investigated in few-electron vertical structures in Ref. [22]. These authors demonstrated that inelastic cotunneling provides a direct and sensitive measure of excited state energies. Here, we use this fact to measure the ST splitting,  $J$ , across the ST transition (for both negative and positive  $J$ ), and for the first time extract two-electron ground state wave function correlations from cotunneling.

Transport through the ST transition has been studied theoretically [12], with a prediction of enhanced Kondo correlations at the ST crossing [13]. Effects of lifting spin degeneracy of the triplet have also been theoretically investigated [14]. For the degenerate triplet case,

a characteristic asymmetric peak in conductance at the ST crossing has been predicted [15, 16]. This predicted asymmetric peak is observed in the present experiment. Previous measurements of ST Kondo effects [10, 11, 23] in dots have not treated the two-electron case.

Measurements were carried out on two similar lateral quantum dots formed by Ti/Au depletion gates on the surface of a GaAs/Al<sub>0.3</sub>Ga<sub>0.7</sub>As heterostructure 105 nm above the 2DEG layer (Fig. 5, inset). The two devices showed similar results; most data are from one of the dots, except those in Fig. 5. The dilution refrigerator base electron temperature was  $T_{el} = 45 \pm 5$  mK, measured from Coulomb blockade peak widths. Differential conductance  $g = dI/dV_{SD}$  was measured with typical ac excitations of  $5 \mu\text{V}$ .

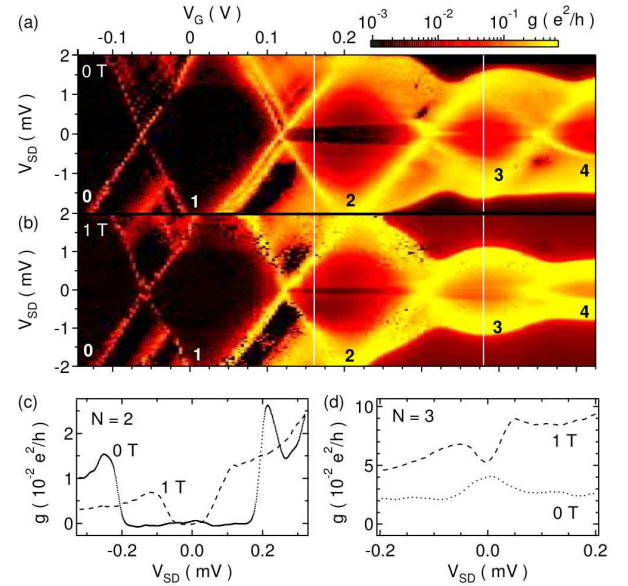


FIG. 1: (a) Differential conductance  $g$  (log color scale) as a function of source-drain bias  $V_{SD}$  and gate voltage  $V_G$  at  $B_{\perp} = 0$ , at base electron temperature  $T_{el} = 45$  mK. Numbers 0 through 4 are number of electrons in the dot. White vertical lines identify the locations for data shown in (c) and (d). (b) Same as (a), at  $B_{\perp} = 1$  T. (c) Differential conductance through the  $N = 2$  diamond showing step with overshoot at  $V_{SD} = J(B_{\perp})/e$  at  $B_{\perp} = 0$  and 1 T. (d) Differential conductance through the  $N = 3$  diamond showing Kondo peak at  $V_{SD} = 0$  for  $B = 0$ , split by  $B_{\perp} = 1$  T.

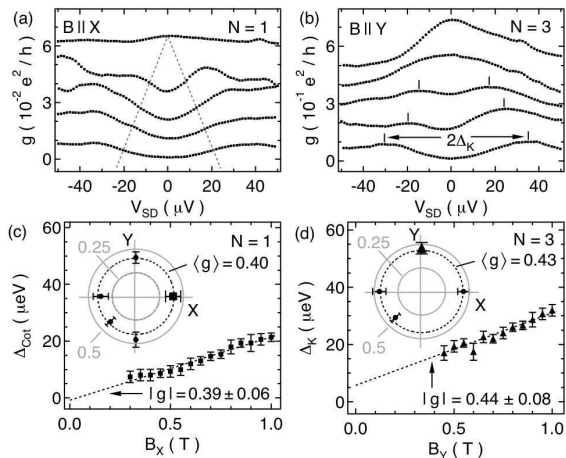


FIG. 2: (a) Differential conductance  $g$  as a function of  $V_{SD}$  in the  $N = 1$  diamond ( $V_G = 0.1$  V) for in-plane fields  $B_X = 0, 0.4, 0.6, 0.8, 1$  T, (top to bottom, curves offset). Dashed grey lines are guides to the eye showing the cotunneling gap. (b)  $g(V_{SD})$  shows a zero-bias peak in the  $N = 3$  valley ( $V_G = 0.42$  V) that splits in an in-plane field  $B_Y = 0, 0.25, 0.45, 0.7, 0.95$  T (top to bottom, curves offset). (c,d) splitting energies (see text) versus magnetic field as in (a,b) with linear fits. Insets: angular dependence of the g-factor in the plane of the 2DEG indicating isotropic behavior. Dashed circles show direction-averaged g-factors. Directions  $X$  and  $Y$  in the plane are arbitrary.

Figures 1(a,b) provide an overview of transport spectroscopy data. Diamond patterns of high conductance correspond to gate voltages  $V_G$  where the ground state of the dot aligns with the chemical potential of either the source or drain, allowing sequential tunneling through the dot [24, 25]. Transport is absent at more negative gate voltages, indicating the absolute occupancy of the dot ( $N = 0$  to 4). Conductance features that vanish below a finite source-drain voltage  $|V_{SD}| = \Delta/e$  involve transport through an excited state at energy  $\Delta$  above the ground state. An example of the latter is the nearly horizontal band running through the center of the  $N = 2$  diamond. Beyond this band transport through the excited triplet channel of the  $N = 2$  dot becomes allowed, as discussed below.

Inside the diamonds, sequential tunneling is Coulomb blocked and transport requires higher order (cotunneling) processes [22, 25]. Elastic cotunneling leaves the energy of the dot unchanged; inelastic cotunneling, which leaves the dot in an excited state, requires energy supplied by the source-drain bias. The inelastic mechanism becomes active above a threshold  $V_{SD}$  and is independent of  $V_G$ .

We first discuss the one-electron regime. A conduction threshold within the  $N = 1$  diamond [Figs. 1(a,b)] emerges from the crossing of ground-state and excited-state sequential tunneling lines [22]. These features correspond to the onset of inelastic cotunneling through the first orbital excited state lying  $\Delta_1 \sim 1.2(1.0)$  meV above the ground state for a field  $B_{\perp} = 0(1)$  T perpendicular to the 2DEG. Measurements with magnetic fields up to 1 T

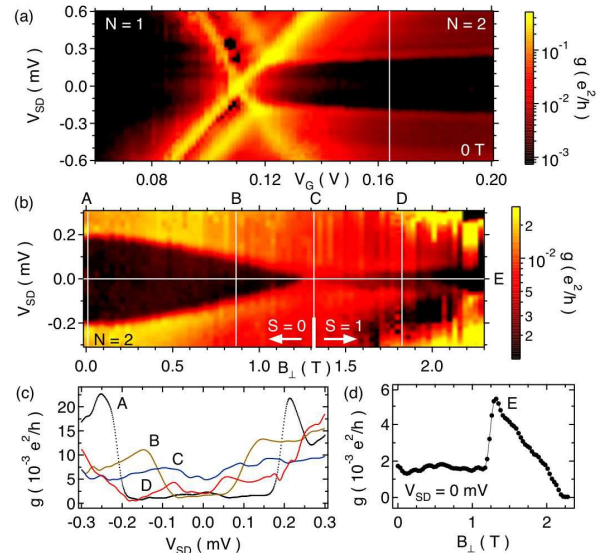


FIG. 3: (a) Differential conductance  $g$  (log color scale) as a function of  $V_{SD}$  and  $V_G$  for  $B = 0$  T in the vicinity of the  $N = 1 \rightarrow 2$  transition. (b)  $g(V_{SD}, B_{\perp})$  at  $V_G = 0.164$  V (vertical white line in (a)) [27] shows the perpendicular field dependence of the singlet-triplet gap. (c) Cuts showing  $g(V_{SD})$  at the positions of the vertical lines in (b), marked A, B, C, D. (d) Horizontal cut (E in (b)) showing  $g(B_{\perp})$  at zero bias. Note the asymmetric peak in  $g$  at the singlet-triplet transition.

along different directions in the plane of the 2DEG show inelastic cotunneling through Zeeman split one-electron states [Fig. 2(a)]. Measurement of Zeeman energies via cotunneling was established in Ref. [26]. The cotunneling gap  $\Delta_{Cot}$ —extracted by taking half the peak splitting of  $dg/dV_{SD}$ —is shown in Fig. 2(c) for one of the field directions. The g-factors are extracted from a linear fit to  $\Delta_{Cot}(B)$  and are found to be isotropic within experimental error, giving a value of  $\langle g \rangle = 0.40 \pm 0.03$  averaged over the measured field directions. This is close to the bulk GaAs value and consistent with previous (few-electron) experiments [1].

For  $N = 3$ , a zero-bias conductance peak, presumably due to the Kondo effect [9], splits in both perpendicular [Fig. 1(d)] and in-plane [Fig. 2(b)] magnetic fields. The splitting  $\Delta_K$  due to in-plane field—taken as half the distance between maxima of the split peaks [indicated in Fig. 2(b)]—is shown in Fig. 2(d) along with a best fitting line. Slopes from the fits do not depend on direction in the plane, and give  $\langle g \rangle = 0.43 \pm 0.03$ , consistent with the one-electron cotunneling data [Fig. 2(c)]. Note that unlike the cotunneling data, the Kondo data does not extrapolate to  $\Delta_K(0) = 0$ , as also reported in previous experiments [26]. The threshold in-plane field  $B_K$  for the appearance of Kondo peak splitting gives an estimate of the Kondo temperature ( $g\mu_B B_K \gtrsim k_B T_K$ ) of  $T_K \sim 150$  mK [26].

A detailed view of two-electron transport is shown in Fig. 3(a). The nearly horizontal band running through the  $N = 2$  diamond [see also Fig. 1(a,b)] corresponds to

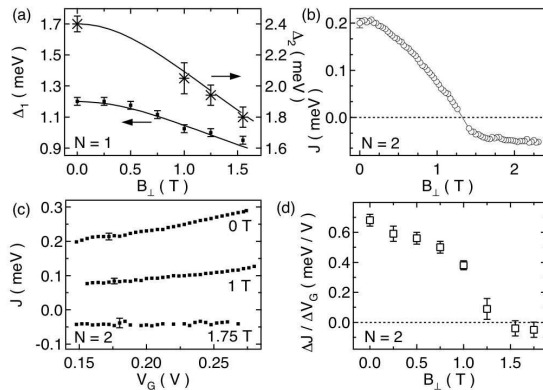


FIG. 4: (a) First and second one-electron excited state energies  $\Delta_1$  and  $\Delta_2$ , measured from sequential tunneling along with fits to a 2D anisotropic harmonic oscillator model with  $\hbar\omega_a = 1.2$  meV and  $\hbar\omega_b = 3.3$  meV (see text). (b) Singlet-triplet splitting  $J$  as a function of magnetic field  $B_\perp$ . (c) Dependence of  $J$  on gate voltage  $V_G$  for various  $B_\perp$  as indicated. (d) Average slopes  $\Delta J(V_G)/\Delta V_G$  from (c) as a function of magnetic field  $B_\perp$ , showing strong reduction of gate voltage dependence of  $J$  at large  $B_\perp$ .

the onset of inelastic cotunneling through the triplet excited state, which becomes active for  $|V_{SD}| > J/e$ . The inelastic cotunneling edges align with the triplet excited state lines seen in sequential tunneling outside the diamond, as expected [22]. We use this cotunneling feature to measure the ST splitting  $J$ . The zero-field value measured here,  $J(B = 0) \sim 0.2$  meV, is much less than the  $N = 1$  orbital level spacing due to strong interactions, consistent with theoretical estimates [18] and previous measurements [5]. A surprising zero-bias conductance peak in the middle of the cotunneling gap, visible in Fig. 3(a) in the range  $0.12 \text{ V} \lesssim V_G \lesssim 0.15 \text{ V}$  is not understood.

Perpendicular field dependence of the ST splitting  $J(B_\perp)$  is investigated by plotting  $g$  along a cut through the  $N = 2$  valley as a function of  $B_\perp$  [Fig. 3(b)]. Near  $B_\perp = B^* \sim 1.3$  T the ST gap closes and then reopens at larger fields. We interpret this as a ST crossing where the triplet state becomes the ground state for  $B_\perp > B^*$  [Fig. 4(b)]. We note that in-plane fields up to 1 T cause no observable change in the two electron spectrum. We also find that  $J$  depends on the gate voltage  $V_G$  [Fig. 4(c)], as observed previously [5, 20], though at larger fields this dependence becomes significantly weaker [Fig. 4(d)]. The zero-bias conductance within the  $N = 2$  diamond as a function of field shows a large, asymmetric peak at  $B_\perp = B^*$  [Fig. 3(d)], consistent with predictions for elastic cotunneling at the ST crossing [16] (see also [15]).

Before turning to wave function correlations, we first extract some useful information about the dot shape from the  $N = 1$  excitation spectrum. Transport spectra for the  $N = 0 \rightarrow 1$  transition, extracted from plots like Fig. 1(a) in the region between the  $N = 0$  and  $N = 1$  diamonds, give first (second) excited state energies lying  $\Delta_{1(2)}$  above the ground state. We find  $\Delta_2 \sim 2\Delta_1$ , indicating roughly

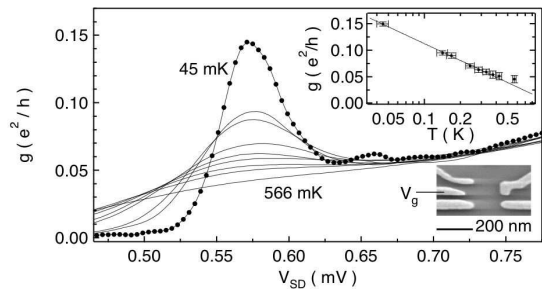


FIG. 5: Differential conductance  $g$  as a function of  $V_{SD}$  for temperatures  $T_{el} = 45, 140, 170, 240, 280, 330, 380, 420, 570$  mK (top to bottom) showing overshoot at  $V_{SD} \sim J/e$ . Inset: peak conductance as a function of temperature with best-fit  $\log(T)$  dependence (line).

harmonic confinement. Dependencies of  $\Delta_{1(2)}$  on perpendicular field are well described by a 2D anisotropic harmonic oscillator model [28]. From zero-field data, we extract  $\hbar\omega_a = 1.2$  meV where  $a(b)$  is along the larger (smaller) dimension of the dot; the energy scale for the smaller direction is found by fitting the field dependence of  $\Delta_1(B_\perp)$ , which gives  $\hbar\omega_b = 3.3$  meV [28]. As a check of these values, good agreement between experimental and predicted values for  $\Delta_2(B_\perp)$  is found [Fig. 4(a)]. We conclude that the dot potential is spatially elongated by a factor of  $\sim 1.6 = \sqrt{\omega_b/\omega_a}$ .

We note that for strong coupling of the dot to the leads, the onset of inelastic cotunneling at  $V_{SD} = J/e$  shows considerable overshoot, as seen in Fig. 5 (measured in a device similar to the one discussed above, with larger ST splitting,  $J(0) \sim 0.57$  meV). The temperature dependence of the maximum overshoot is shown in the inset of Fig. 5 along with a line indicating a Kondo-inspired  $\log(T)$  dependence [10, 11, 23]. The FWHM of the corresponding positive peak in  $dg/dV_{SD}$  is proportional to  $T$  at high temperatures and saturates at  $T \sim 80$  mK, giving an estimate of  $T_K$  for this device. However, a quantitative theory of nonequilibrium ST Kondo effect would be needed to further analyze these data.

Finally, we investigate correlations in the two-electron wave function following the analysis of Ref. [16]. We note that Ref. [16] specifically considers a two-electron *double* quantum dot; we anticipate that the elongated shape of our single dot will lead to a spatially separated charge arrangement for  $N = 2$ , not unlike a double dot in the limit of strong interdot coupling. Selecting basis states appropriate for a double dot but applicable here as well—i.e., symmetric ( $|+\rangle$ ) and antisymmetric ( $|-\rangle$ ) states along the long axis of the dot—we identify  $|+\rangle$  and  $|-\rangle$  with the orbital ground and first excited states of the one-electron dot. Because of electron-electron interactions, the  $N = 2$  ground-state singlet generally comprises an admixture of the one-electron ground and excited orbital states. The amount of admixed excited state  $|-\rangle$  is parameterized by  $\phi$  ( $0 \leq \phi \leq 1$ ), the so-called interaction parameter. Knowing  $\phi$  allows two other important quantities to be

extracted: the double occupancy,  $D = (1 - \phi)^2 / 2(1 + \phi^2)$ , and the concurrence [29],  $c = 2\phi / (1 + \phi^2)$ , which respectively parameterize correlations and entanglement of the two-electron singlet ground state [16].

To extract  $\phi$  from elastic cotunneling data, one also needs to know the charging energy for adding the second electron, the operating position within the  $N = 2$  diamond, and the couplings to each lead for both the singlet and the triplet,  $\Gamma_{1,2}^{S,T}$ . At fields well below the ST transition, these  $\Gamma$ 's can be estimated from excitation spectra at the  $N = 1 \rightarrow 2$  transition by fitting a thermally broadened Lorentzian to the tunneling lines [30]. Upon inserting these quantities into Eqs. 8 and 10 of Ref. [16], we find  $\phi \sim 0.5 \pm 0.1$ , indicating that the  $N = 2$  ground-state singlet contains a significant admixture of the excited one-electron orbital state due to electron-electron interactions. We emphasize that this method does not rely explicitly on a double dot interpretation [31]. From this value of  $\phi$  we extract a concurrence of  $c \sim 0.8$  for the two-electron singlet. This is close to the maximum concurrence value  $c = 1$ , which characterizes a pair of singlet-correlated electrons in fully non-overlapping or-

bit states.

Two alternative methods for estimating  $\phi$  give consistent results with the cotunneling method. First, one may adapt the formula  $\phi = \sqrt{1 + (4t/U)^2} - 4t/U$  from [16] by associating the measured  $\Delta_1$  with the tunnel splitting  $2t$  of the two lowest noninteracting single-particle states, and the charging energy to add the second electron with  $U$ . The second alternative method uses the size of the elastic cotunneling step at the ST transition [see Fig. 3(d)] which is shown to be related to  $\phi$  in [16]. It is notable that all three methods allow the concurrence, a measure of “useful” (i.e., spatially separated) two-particle entanglement, to be extracted from a dc transport measurement.

We thank Daniel Loss for numerous contributions to this work. We also thank M. Eto, L. Glazman, V. Golovach, W. Hofstetter, and M. Stopa for valuable discussion. This work was supported in part by DARPA under the QuIST Program, the ARDA/ARO Quantum Computing Program, and the Harvard NSEC. Work at UCSB was supported by QUEST, an NSF Science and Technology Center.

small

- 
- [1] R. Hanson et al., Phys. Rev. Lett. **91**, 196802 (2003); R. M. Potok et al., Phys. Rev. Lett. **91**, 16802 (2003); J. M. Elzerman et al., App. Phys. Lett. **84**, 4617 (2004).
  - [2] S. Tarucha et al., Phys. Rev. Lett. **77**, 3613 (1996).
  - [3] L. P. Kouwenhoven et al., Science **278**, 1788 (1997).
  - [4] Bo Su et al., Phys. Rev. B **46**, 7644 (1992); R. C. Ashoori et al., Phys. Rev. Lett. **71**, 613 (1993); T. Schmidt et al., Phys. Rev. B **51**, 5570 (1995).
  - [5] J. Kyriakidis et al., Phys. Rev. B **66**, 35320 (2002).
  - [6] T. Fujisawa et al., Nature **419**, 278 (2002); T. Fujisawa et al., J. Phys.: Cond. Mat. **15**, R1395 (2002).
  - [7] V. N. Golovach et al., Phys. Rev. Lett. **93**, 16601 (2004).
  - [8] J. M. Elzerman et al., Nature **430**, 431 (2004).
  - [9] D. Goldhaber-Gordon et al., Nature **391**, 156 (1998); S. M. Cronenwett et al., Science **281**, 540 (1998).
  - [10] S. Sasaki et al., Nature **405**, 764 (2002).
  - [11] J. Schmid et al., Phys. Rev. Lett. **84**, 5824 (2000); W. G. van der Wiel et al., Phys. Rev. Lett. **88**, 126803 (2002); C. Fühner et al., Phys. Rev. B **66**, 161305 (2002).
  - [12] M. Wagner et al., Phys. Rev. B **45**, 1951 (1992), D. Pfannkuche et al., Phys. Rev. B **47**, 2244 (1993), P. Hawrylak, Phys. Rev. Lett. **71**, 3347 (1993).
  - [13] M. Eto and Yu. V. Nazarov, Phys. Rev. Lett. **85**, 1306 (2000); M. Pustilnik and L.I. Glazman, *ibid.*, 2993.
  - [14] D. Giuliano and A. Tagliacozzo, Phys. Rev. Lett. **84**, 4677 (2000); M. Eto and Yu. V. Nazarov, Phys. Rev. B **64**, 85322 (2001); M. Pustilnik and L.I. Glazman, *ibid.*, 45328.
  - [15] W. Hofstetter and H. Schoeller, Phys. Rev. Lett. **88**, 16803 (2001); M. Pustilnik et al., Phys. Rev. B **68**, R161303 (2003).
  - [16] V. N. Golovach and D. Loss, Europhys. Lett. **62**, 83 (2003); Phys. Rev. B **69**, 245327 (2004).
  - [17] S. M. Reimann et al., Rev. Mod. Phys. **74**, 1283 (2002).
  - [18] G. Burkard et al. Phys. Rev. B **59**, 2070 (1999).
  - [19] D. Loss and D. P. DiVincenzo, Phys. Rev. A **57**, 120 (1998).
  - [20] A. Kogan et al., Phys. Rev. B **67**, 113309 (2003).
  - [21] A. Fuhrer et al., Phys. Rev. Lett. **91**, 206802 (2003); S. Tarucha et al., Phys. Rev. Lett. **84**, 2485 (2000).
  - [22] S. De Franceschi et al., Phys. Rev. Lett. **86**, 878 (2001); M. R. Wegewijs and Yu. V. Nazarov, cond-mat/0103579.
  - [23] J. Nygard et al., Nature **408**, 342 (2000). W. Liang et al., Phys. Rev. Lett. **88**, 126801 (2002).
  - [24] Density of states modulations in the leads, here due to nanostructures adjacent to the dot, can give additional weak diagonal lines (see for example  $V_{SD} > 0$ ,  $V_G \sim -0.05$  V).
  - [25] I. L. Aleiner et al., Phys. Rep. **358**, 309 (2002).
  - [26] A. Kogan et al., cond-mat/0312186.
  - [27] The gate voltage of the cut,  $V_G^{\text{cut}}(B)$ , was adjusted to compensate for a diamagnetic shift in gate voltage of the overall diamond pattern. Gate voltages ranging from  $V_G^{\text{cut}}(0) = 0.164$  V to  $V_G^{\text{cut}}(2 \text{ T}) = 0.179$  V are determined by holding fixed the position of the cut within the diamond pattern.
  - [28] B. Schuh, J. Phys. A: Math. Gen. **18**, 803 (1985).
  - [29] J. Schliemann et al., Phys. Rev. B **63**, 85311 (2001).
  - [30] E. B. Foxman et al., Phys. Rev. B **50**, 14193 (1994).
  - [31] V. Golovach and D. Loss, private communication.